



Application of continuous wavelet transform based on Fast Fourier transform for the quality analysis of arc welding process

Vikas Kumar¹ · Subhadip Ghosh¹ · Manoj Kumar Parida¹ · Shaju K. Albert²

Received: 9 May 2022 / Revised: 12 July 2023 / Accepted: 12 September 2023 / Published online: 25 September 2023

© The Author(s) under exclusive licence to The Society for Reliability Engineering, Quality and Operations Management (SREQOM), India and The Division of Operation and Maintenance, Lulea University of Technology, Sweden 2023

Abstract SMAW (Shielded Metal Arc Welding) and GMAW (Gas Metal Arc Welding) are two of the most prominent welding processes commonly utilized in almost all types of modern industries. Among various aspects of these processes, some of the important parameters that govern the quality of the final weld product are the skill level of welders, welding consumables, and the role of shielding gases (in GMAW). Currently, the role of these parameters in determining the quality of the welded product is examined by evaluating the final weld produced and not by investigating how these factors affect the welding process. This is an indirect way to evaluate such welding parameters, which are both time-consuming and expensive. During the actual welding process, random variations in arc signals (voltage and current) take place. These dynamic variations are so short and rapid that ordinary ammeters and voltmeters cannot monitor the rate of such variations. However, the reliable acquisition of such variations and its subsequent analysis can provide very useful information in determining the quality of the final weld product. In this study, arc voltage and current were acquired at 100,000 samples/sec, filtered and subsequently analyzed using Continuous Wavelet Transform based on Fast Fourier Transform (CWT-FFT) technique to evaluate welding skill, welding electrodes (in SMAW process), and the effect of shielding gases (in GMAW process). Results thus obtained clearly differentiated the skill level of different trainee welders and welding electrodes in the SMAW process and the effect of shielding gases and arc

current in the GMAW process. Very good correlation among the obtained results, its weld bead and its weld pool images were observed. Hence, this research proposes a simple yet effective methodology to evaluate the arc welding process parameters using CWT-FFT analysis of the welding signals.

Keywords Continuous wavelet transforms · Signal processing · Arc welding · Welding skill · Metal transfer · Shielding gas

1 Introduction

Arc welding is one of the most commonly and widely used welding processes in almost all types of modern industries for joining various ferrous and non-ferrous metals. Due to its inherent advantages it has like the ease of use, versatility, flexibility, and low maintenance cost this process finds its application in fabricating almost everything we see around us like buildings, bridges, locomotives & coaches, general machinery, defense equipment etc. This process has many variants and the primary differences between these processes are the methods by which the molten metal is protected from the atmosphere (Ador welding limited 2008). The stochastic nature of arc welding, caused by its unpredictable arc behavior and intricate metal transfer modes, led to the observation of dynamic fluctuations in arc voltage and current during the actual welding process. The quality of the final weld product depends heavily on several welding parameters that create these random fluctuations. Consequently, if these variations that occur during the actual welding process are suitably acquired and processed then, the effect of various arc welding parameters like the skill of welders, the role of shielding gases and consumables etc. on the final weld product can be understood in a much better way than it is done at present

✉ Vikas Kumar
iamvikasjha@gmail.com; vikas.jhafet@kiit.ac.in

¹ School of Electronics Engineering, Kalinga Institute of Industrial Technology, Bhubaneswar, India

² Metallurgy & Materials Group, Indira Gandhi Centre for Atomic Research, Kalpakkam, India

method. However, such dynamic variations in arc voltage and current occur for very short intervals of time. Therefore, to record such variations, a high-speed data acquisition and monitoring system (along with relevant sensors), capable of acquiring arc variations, at the same rate as they occur should only be used. To establish an effective weld monitoring system, diverse techniques have been employed. Some researchers have utilized visible light imaging, using schlieren imaging for examining gas shield flow in GMAW (Bitharas et al. 2018) or spectroscopic parameters for on-line monitoring (Mirapeix et al. 2009). Similarly, voltage sensing techniques have been harnessed for weld penetration sensing in pulsed gas tungsten arc welding (Zhang et al. 2016), combined with other sensors for penetration prediction (Chen and Chen 2010), and for detecting welding defects in conjunction with arc spectrum and sound (Zhang et al. 2015). Furthermore, acoustic emission techniques such as the "Gorbunov effect" have facilitated remote testing of welding flaws (Kapranov and Sutorikhin 2017), while another research combined acoustic emission with air-coupled ultrasonic testing for real-time weld quality assurance in GTAW (Zhang et al. 2019). Vision sensing, meanwhile, has also proven beneficial. Researchers have developed a narrow-seam identification algorithm for precision in TIG welding (Zhang et al. 2018), and proposed a three-dimensional system using structured light to navigate dynamic welding challenges (Song and Zhang 2007). These systems rely on diverse processing units, including Field Programmable Gate Arrays (FPGA) (Lanzoni et al. 2010), Microprocessors (Luksa and Rymarski 2006), Microcontrollers (Lebar et al. 2012), System on Chips (SoCs) (Kumar et al. 2020), and Analog to digital cards (Siewert et al. 2002). Lately, even the common Digital Storage Oscilloscope (DSO) has found utility in this field (Kumar et al. 2018a).

Weld data obtained from monitoring systems have been evaluated using various techniques, such as the statistical analysis of high-speed voltage data in GMAW for skill assessment (Kumar et al. 2018a), a method involving pool image centroid deviation for precise seam tracking in arc welding (Li and Gao 2014), and the application of independent component analysis to detect short arc welding faults (Li and Simpson 2009). This is supplemented by Artificial Neural Network (ANN) techniques, including a real-time, Deep Neural Network (DNN) based method for predicting porosity defects without additional devices (Shin et al. 2020), the utilization of data mining, machine learning, and deep learning techniques for enhanced decision-making and process control in welding (Martínez and Alfaro 2020), and a unified deep neural network for superior weld defect classification (Yang and Jiang 2020). Furthermore, several signal processing techniques like Short Time Fourier Transforms (STFT), Fourier Transform (FT), etc. were also extensively employed to enhance the reliability of the welding signal (Kumar et al.

2018a). But, FT and STFTs have the limitations of localization of frequency components (Komorowski and Pietraszek 2015). Therefore, other advanced signal processing algorithms like Continuous Wavelet Transform (CWT) and Discrete Wavelet Transforms (DWT) are widely adopted in the literature to process the non-stationarity of welding signals (Chen and Lv N, 2014). In parallel, industries utilizing induction motors have leveraged condition monitoring systems that can detect faults amidst power quality issues, utilizing techniques like DWT for signal decomposition and feature extraction (Das et al. 2016).

Wavelet transforms are essentially a Multi-Resolution analysis (MRA) technique that can be used to obtain the time–frequency representation of the Welding signal. MRA is designed to give good time resolution and poor frequency resolution at high frequencies and good frequency resolution and poor time resolution at low frequencies (Das et al. 2016). Chen et. al (2014) has developed a wavelet-based algorithm to extract Al alloy weld pool in the GTAW process and subsequently proposed the idea of intelligentized welding manufacturing technology. Das et. al in (2016) have used the wavelet transform technique to identify tunnel type of defects in an FSW process and for this, the authors have analyzed the real-time force signal by amalgamating the properties of wavelet and Hilbert-Huang transform. Pal et. al (2010) have used the wavelet transform to generate accurate signal features to train an ANN model for predicting the weld joint strength in a pulsed metal inert gas welding process. The denoising property of wavelet transforms has also been harnessed extensively for weld quality analysis. For example, a wavelet transform-based denoising algorithm was proposed for the Gas Tungsten Arc Welding (GTAW) process (Lv et al. 2013). Likewise, other studies have utilized this property to tackle power quality issues in industrial plants, identify transient events, and categorize disturbances. At the same time, power quality disturbances have been detected and classified under noisy environments using innovative signal processing tools such as fusion of time domain descriptors (FTDD), improving mitigation strategies (Zhou et al. 2001). Innovative methods like Linear Mode Decomposition and Continuous Wavelet Transform have been deployed, demonstrating effectiveness in rectifying distortions in square wave Alternating Current (AC) welding signals and in extracting stationary attributes from non-stationary welding data (Yu et al. 2005). These techniques have enabled noise reduction within welding signals (He et al. 2016), facilitating the extraction of diverse process parameters pivotal to enhancing welding process evaluations (Caglar 2012).

From the above discussion, it is clear that the wavelets can be effectively used to process the non-stationarity of the welding signals. But it is important to note that for large data sets the computation of wavelet coefficients

are both time and resource-consuming. Additionally, none of the works of literature has attempted the evaluation of other important welding parameters like welding skill, welding consumables, the role of shielding gases etc. using continuous wavelet transforms based FFT techniques. In the present study, we conducted an in-depth analysis and investigation of welding signals including arc voltage, current, and weld pool imagery that were acquired by employing a high-speed Digital Storage Oscilloscope (DSO) and an advanced imaging apparatus. Our research primarily focused on evaluating the proficiency of welders, examining the characteristics of welding electrodes in the Shielded Metal Arc Welding (SMAW) process, and investigating the impact of shielding gases in Gas Metal Arc Welding (GMAW). In an effort to discern intricate complexity within the welding data, we deployed advanced statistical methodologies in conjunction with the Continuous Wavelet Transform predicated on the Fast Fourier Transform (CWT-FFT) technique. The subsequent section, Sect. 2, delineates on the CWT-FFT technique, illuminating its mathematical underpinnings and establishing its aptness for analyzing intricate welding data. Section 3 chronicles a comprehensive delineation of our experimental arrangement, encapsulating the setup of the data procurement experimental apparatus, execution of the welding procedures, and the array of equipment engaged. This section meticulously describes every stage, from the complexities of data capturing to the rigorous implementation of the welding protocols. Section 4 serves as the exposition of our study’s compelling discoveries, bolstered by insightful discourse. This section is judiciously divided into three segments: 4.1 Evaluation of Welding Skill, 4.2 Assessment of Welding Consumable, and 4.3 The Implication of Shielding Gases in the GMAW Procedure. Each segment reveals fascinating insights related to distinct facets of the welding operation and conducts an in-depth exploration of their repercussions. Finally, in the Conclusion section, we briefly encapsulate the paramount findings of our study, underscoring their relevance within the sphere of arc welding quality analysis. Furthermore, we emphasize the salient contributions of our study and extend recommendations for future explorations, thereby encouraging further progress in this esteemed discipline.

2 CWT-FFT based methodology

CWT essentially represents the correlation between continuous input signal “ $x(t)$ ” and a suitable wavelet function shown below.

$$Cw(a, b) = \int_{-\infty}^{+\infty} x(t)\psi_{a,b}^* dt$$

$$= \frac{1}{\sqrt{a}} \int_{-\infty}^{+\infty} x(t)\psi^*\left(\frac{t-b}{a}\right) dt \tag{1}$$

Here, $\psi_{(t)}^*$ represents the complex conjugate of original mother wavelet $\psi(t)$ (Torrence and Compo 1998), $Cw(a,b)$ is a function of the wavelet’s dilation “ a ” and translation “ b ” parameters (Rioul and Vetterli 1991). The energy normalized factor $\frac{1}{\sqrt{a}}$ is an integral coefficient (Komorowski and Pietraszek 2015). However, a wavelet must have finite energy as per the following mathematical criteria

$$E = \int_{-\infty}^{+\infty} |\psi(t)|^2 dt < \infty \text{ and } C_{\psi} = \int_{-\infty}^{+\infty} \frac{|\psi^{\wedge}(\omega)|^2}{\omega} d\omega < \infty \tag{2}$$

$$\hat{\psi}(\omega) = \int_{-\infty}^{+\infty} \psi(t)e^{-i\omega t} dt \tag{3}$$

Where ω represents angular frequency and $\psi(\omega)$ is the Fourier transform of mother wavelet $\psi(t)$. The condition presented with Eq. (2) and (3) is also known as the condition of admissibility and generally based on how fast $|\psi^{\wedge}(\omega)|^2$ tends to zero compared to $\frac{1}{\omega}$. This condition implies that $\hat{\psi}(\omega) = 0$ and that the wavelet has no frequency component. C_{ψ} refers to admissibility constant whose value essentially depends on the type of chosen wavelet (Rioul and Vetterli 1991). The CWT thus obtained results in a two-dimensional scalogram function $E(a, b) = |C_w(a, b)|^2$ depicting the energy distribution as a function of scales “ a ” and positions “ b ”. Using Eq. 4 scale “ a ” can be transformed to frequency of wavelet “ f_a ”. This clearly indicates that at $a = 1$ and $b = 0$, the wavelet’s associated frequency becomes the mother wavelet’s characteristic frequency. Therefore the f_c used in a CWT essentially indicates the whole frequency content in the wavelet and unlike Fourier analysis in CWT the signal is not decomposed of numerous sinusoidal frequencies (Torrence and Compo 1998).

$$f_a = \frac{f_c}{a} \tag{4}$$

Since, Eq. 5 describes the inverse wavelet transform, it should be able to reconstruct the original signal if the wavelet coefficients are known. Here, K_{ψ} is constant whose value is determined by the type of wavelet similarly, $D(a, t)$ is the details function whose value is given by Eq. (6).

$$x(t) = \frac{1}{K_{\psi}} \int_{a=0}^{+\infty} \left(\int_{b=-\infty}^{+\infty} Cw(a, b)\psi_{a,b}(t) \frac{db}{a^2} \right) da$$

$$= \frac{1}{K_{\psi}} \int_0^{+\infty} D(a, t) da \tag{5}$$

$$D(a, t) = \int_{b=-\infty}^{+\infty} \frac{1}{a^2} Cw(a, b) \psi_{a,b}(t) db \tag{6}$$

For most of the practical applications, wavelet series or wavelet coefficients are used to reconstruct the original and this in turn heavily depends on the selection of appropriate wavelet function. The classical CWT presented till now is time consuming and requires high computing resources for its operation. Hence, in recent years modified and efficient way to compute CWT using FFT algorithms have evolved (Rioul and Vetterli 1991) by simply re-defining the CWT of Eq. 1 to Eq. (7).

$$Cw(a, b) = \int_{-\infty}^{+\infty} x(t) \psi_{ab}^*(t) dt = \int_{-\infty}^{+\infty} x(t) \psi_a^*(b - t) dt \tag{7}$$

where,

$$\psi_a(t) = \frac{1}{\sqrt{a}} \psi\left(\frac{t}{a}\right) \text{ and } \psi_{ab}(t) = \frac{1}{\sqrt{a}} \psi\left(\frac{t-b}{a}\right) \tag{8}$$

It is evident from Eqs. 7 and 8 that CWT is now just a simple convolution of the signal with the wavelet (Rioul and Vetterli 1991). As a result, a CWT can be considered an inverse Fourier transform.

$$Cw(a, b) = \frac{1}{2\pi} \int_{-\infty}^{+\infty} \hat{x}(\omega) \hat{\psi}_{a,b}^*(\omega) d\omega \tag{9}$$

where, $\hat{\psi}_{a,b}^*(\omega) = \sqrt{a} \hat{\psi}^*(a\omega) e^{i\omega b}$ indicates the Fourier transform of the processed wavelet and $\hat{x}(\omega) = \int_{-\infty}^{+\infty} x(t) e^{-i\omega t} dt$ is the Fourier transform of the signal $x(t)$.

The methodologies described above were used to analyze the arc welding signal to evaluate various arc welding

parameters. As described in Komorowski and Pietraszek (2015), in the present work also, the calculations were performed using different wavelets i.e., Derivative of Gaussian, Morlet and Paul etc. Additionally, all the available wavelet types were examined using the MATLAB version (2016a). From the rigorous analysis of the wavelets and their properties the non-analytic Morlet wavelet with zero mean was chosen as a candidate wavelet for our present study as its scalogram provided similar information consistent with the known process parameters of an arc welding process (i.e., short circuit metal transfer duration etc.) (Kumar et al. 2018a).

3 Experimental setup

Figure 1 shows the complete schematic of the experimental setup used in this study. The setup used basically comprises of a data acquisition, welding and a high-speed camera setup. Brief descriptions about these modules are given below.

3.1 Data acquisition setup

For all our studies data acquisition was carried out to acquire the instantaneous values of voltage and current by maintaining an identical condition while making bead-on-plate welding on a carbon steel plate using suitable welding consumables. In order to acquire the arc voltage and current, a general-purpose Digital Storage Oscilloscope (DSO7054B) of Agilent Technologies (now Keysight) having a maximum sampling rate of 4 GSa/seconds and bandwidth of 500 MHz was used. DSO7054B has 4 channels with inbuilt AC to DC

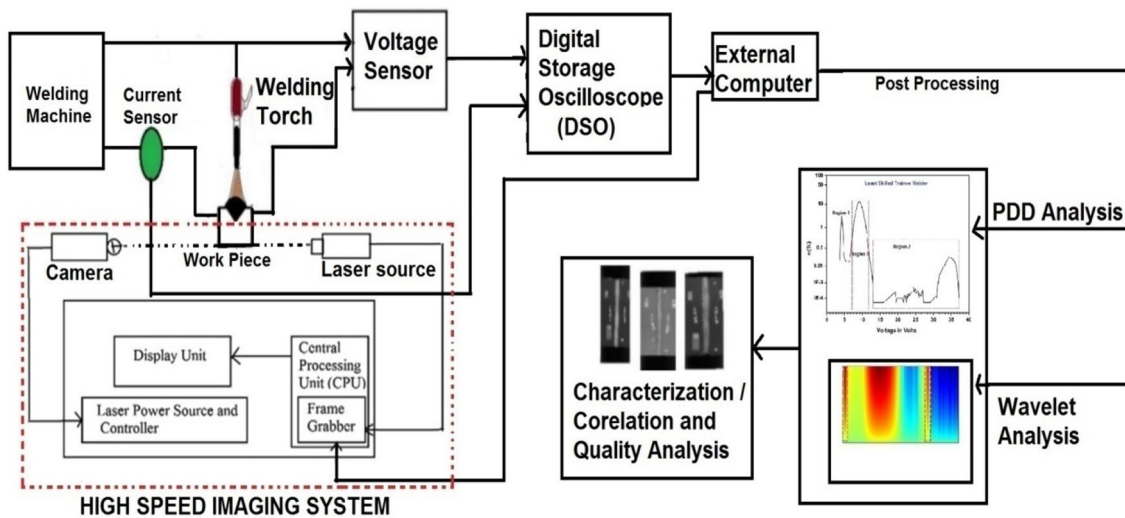


Fig. 1 Schematic of the complete experimental setup

coupling. The input impedance of DSO was 50–1 M Ω and an in-depth memory of 8 M-Points. For sensing welding current, Hall Effect based highly sensitive current clamp (600 A DC and 100 A AC) was used. Similarly, in order to sense arc voltage, a differential probe having 500 MHz bandwidth was used. To achieve high Common Mode Rejection Ratio (CMRR) and to match the overall frequency and attenuation response two signal paths along the measurement were provided. The system has an input capacitance of 2.5 pF and a propagation delay of 6.1 ns. Welding duration was set to 20 s and arc voltage and current were acquired at 100,000 samples /seconds. The acquired data were then filtered for noise and in turn used for subsequent analysis.

3.2 Welding setup

To evaluate the welding skill in the SMAW process, instantaneous current and voltage values were recorded by making bead-on-plate welds on carbon steel using an inverter power source and E 7018 electrodes of 3.15 mm diameter. Similarly, in order to compare different welding electrodes by comparing their arc characteristics welding data were acquired from bead on plate welds on carbon plates using basic coated (E 7018, 3.15 mm diameter) and cellulose coated electrodes (E 6010 of 2.5 mm diameter) and an inverter power source.

Table 1 Composition of shielding gases used in GMAW process

Gas composition	Set current
80% Ar and 20% Co ₂	(a) 200 A (b) 220 A (c) 300 A
100% Ar	(a) 190 A (b) 220 A (c) 240 A
100% Co ₂	(a) 150 A (b) 200A

To investigate the effect of shielding gases in the GMAW process bead-on-plate welding on carbon plate using AWS ER 70S2 wires (of 1.2 mm diameter) were made by varying the shielding gas and current combinations as shown in Table 1. From this table, it can be seen that for each shielding gas, three different current combinations were used to obtain different modes of metal transfer. It should be noted that all welds are prepared using the same welder and machine.

3.3 High speed camera setup

To visualize the metal transfer behavior of welding electrodes and correlate the same with the acquired electrical signal a Fastcam MC2.1 photon focus high speed camera with suitable filters and illumination were used. This camera setup had a maximum capture speed of 10,000 frames/sec with the minimum shutter opening time of 1/100,000 s. Please note that in this study, metal transfer images of various welding electrodes were captured at 5000 frames/sec. Photograph of the DSO based high speed data acquisition, welding and high-speed camera imaging setup is shown in Fig. 2.

4 Results and discussion

4.1 Evaluation of welding skill

Figure 3 depicts the time domain analysis of an unskilled and a skilled trainee welder, in this figure steady-state voltage values and sharp dips from this steady-state can be easily noticed (only 500 ms data are shown for clarity purpose). The sudden decrease in voltage values actually corresponds to the short circuit mode of metal transfer in the molten weld

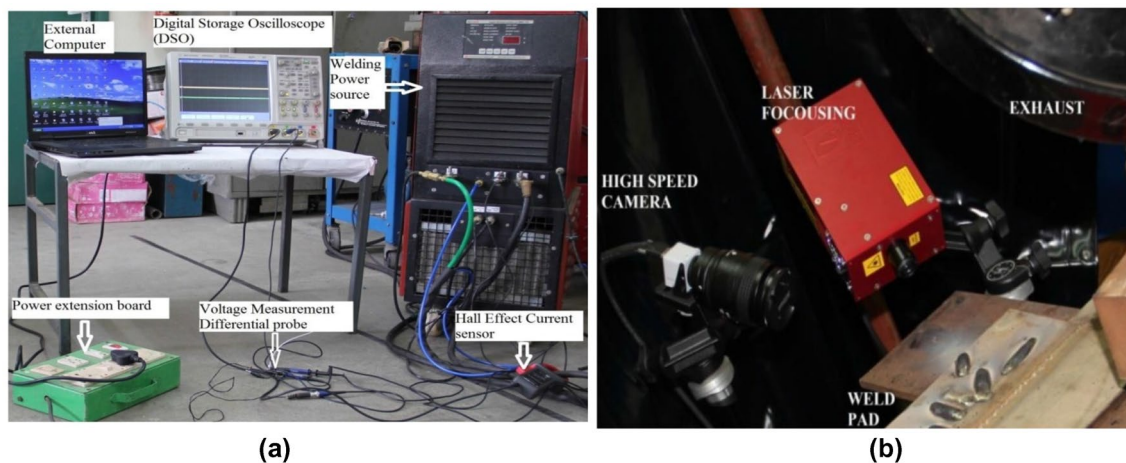


Fig. 2 Photograph of **a** the weld data acquisition setup and **b** high speed camera setup

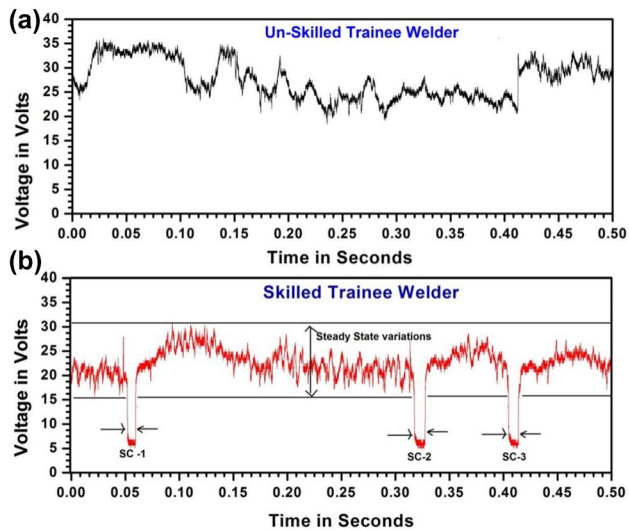


Fig. 3 Time domain oscillogram of **a** Unskilled and **b** skilled welder

pool from an E 7018 (basic type) welding electrode (Kumar et al. 2018a). A careful comparison of Fig. 3a, b reveals that the voltage fluctuations in the oscillogram of an unskilled welder are more than that of a skilled welder. The un-skilled welder has not learnt the welding skill yet and therefore finding it difficult to maintain a constant arc gap. Contrary, a skilled welder knows how to perform steady-state welding and therefore lesser variations with frequent short circuit metal transfers (SC1, SC2 etc.) can be easily noticed.

Probability Density Distribution (PDD) (Kumar et al. 2020) plot of the voltage signal acquired using an unskilled and skilled welder and E7018 electrode used to plot Fig. 3 is shown in Fig. 4. From this figure it is clear that, in general,

the voltage PDD will have three distinct regions (region 1 to region 3), region 1 will be around low voltages, whereas region 2 will be around the mid voltage values. The mid voltage values around region 2 actually correspond to the mean voltages displayed by the voltmeter of the welding power source whereas region 1 indicates the short circuit metal transfer happening in welding pool with E 7018 electrodes. Similarly, region 3 of the voltage PDD (towards the higher voltages) corresponds to the hand stability of the trainee welder to maintain a uniform arc gap. Figure 4b shows the voltage PDD made by a skilled welder, from this figure it is clear that for a good weld made with E 7018 type of basic electrode, voltage PDD should have two distinct and widely separated regions 1, 2 and should have least variations in region 3 (Fig. 4b). On the other hand, the voltage PDD obtained from an unskilled welder in Fig. 4a reveals that an untrained welding personal will have significantly lesser values of region 1 and 2 with large random variations in region 3 (Fig. 4a). Therefore, it is clear that a good welder must have wider region 2 (steady state welding duration) and narrower region 3 (duration of unstable welding). To validate the hypothesis presented just now the bead image and its corresponding radiographs (for skilled and unskilled welders) are shown in Fig. 5. Comparing, Figs. 4 and 5, it is now indeed clear that for a good weld, the welding duration of region 2 must be as wide as possible because wider region 2 ensures more voltage values at steady-state and consequently lesser arc gap variations. Similarly, to ensure stable arc gap variations the duration of region 3 must be as small as possible. Based on the explanations presented above, the durations of region 2 and 3 were evaluated using the CWT based FFT methodology described in Sect. 3.

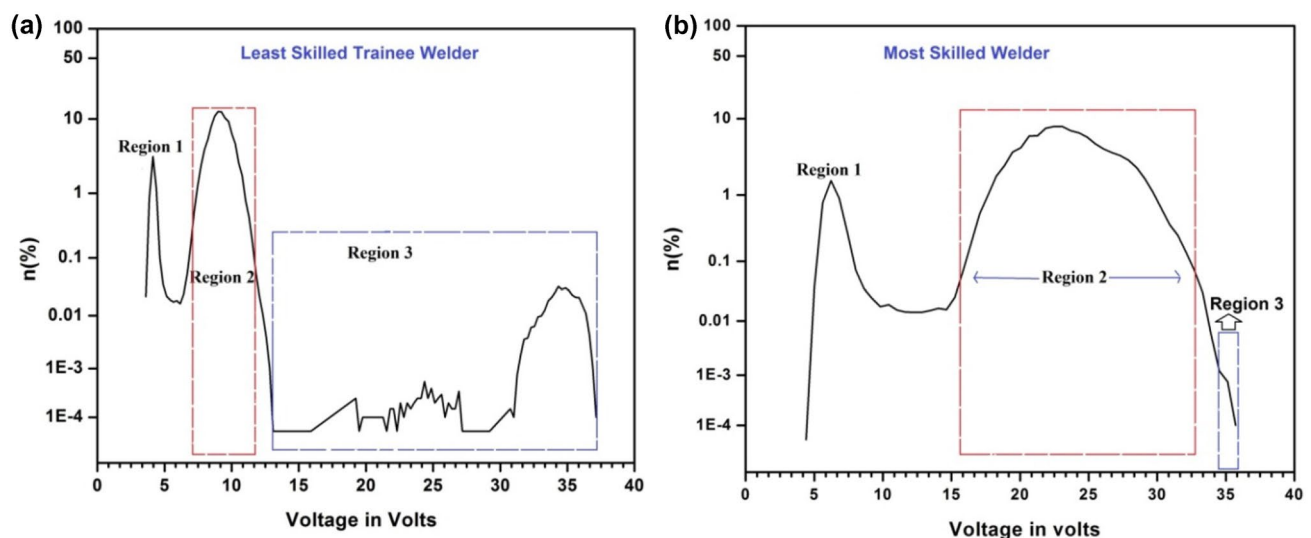


Fig. 4 PDD analysis of **a** Unskilled and **b** skilled welder

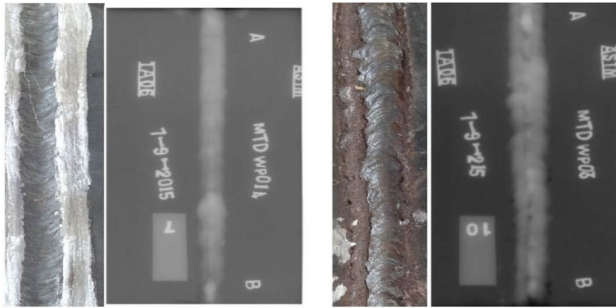


Fig. 5 Bead image and radiographs of (1) skilled and (2) Unskilled welder

Figure 6 represents the scalogram (described in Sect. 3) of the voltage PDD of the skilled and unskilled welder (same welders used to plot Fig. 3 and 4), from this figure one can easily note that the welding duration of region 2 (~ 11 s) for the skilled welder is far greater than the Region 2 duration (~ 4 s) for unskilled welder. Similarly, region 3 duration for skilled welder was around 1 s and the duration of the same for the unskilled welder was nearly 14 s. The analysis just now presented clearly differentiated the skill level of skilled and un-skilled welder and gives us the flexibility to grade the skill levels of trainee welders by monitoring the durations of two regions of the voltage PDD using CWT-FFT technique for any welder.

To confirm the results obtained above in grading the skill levels of trainee welders, a similar analysis needs to be performed on larger sets of trainee welders. Therefore, 20 passing out trainee welders from a weld training institute were examined by monitoring the welding durations of regions 2 and 3 as proposed above and their corresponding rankings are tabulated in Table 2. The proposed rankings using the CWT-FFT technique were correlated with the rankings obtained by monitoring the shift in the voltage PDDs of

the trainee welders with respect to the experienced trainer welder and by performing the visual examinations of their final weld bead (Kumar et al. 2018a). From this table and referring to Fig. 7, a very good correlation between the proposed and current practice of weld skill classification were noticed.

4.2 Evaluation welding consumable

For evaluating the welding electrodes high-speed data acquisition and camera setup described in Sect. 3 was used to acquire welding voltage and current and to capture the metal transfer behavior in E 7018 and E 6010 types of welding consumables. The high-speed camera image in Fig. 8 depicts the metal transfer behavior in such electrodes, it is observed that in E 7018 types of basic electrodes short circuit types of metal transfer is predominant whereas in cellulosic electrodes (E 6010 types), both short circuit and spray modes of metal transfer were noticed. This observation was in agreement with those reported in Kumar et al. 2018a. To study the arc behavior of the individual electrodes their metal transfer characteristics were correlated with their voltage PDDs (Fig. 8). In this correlation, the region of short circuit and spray transfer in E 7018 and E 6010 electrodes respectively can be easily seen.

CWT-FFT algorithm was also used on the voltage PDDs of E 7018 and E 6010 electrodes to quantify their metal transfer durations happening in the actual process. From the CWT-FFT scalogram of the voltage PDD in Fig. 8 obtained from these electrodes, one can easily assess the duration of metal transfer of the individual electrodes. A careful analysis of this figure reveals that for E 7018 the duration of the short circuit mode of metal transfer is nearly 2 s whereas in E 6010 electrodes the same is found to be approximately 1 s. Similarly, in addition to the short circuit, the duration of spray mode of metal transfer happening only in E 6010

Fig. 6 CWT-FFT analysis of the voltage PDD of (1) skilled and (2) Unskilled welder

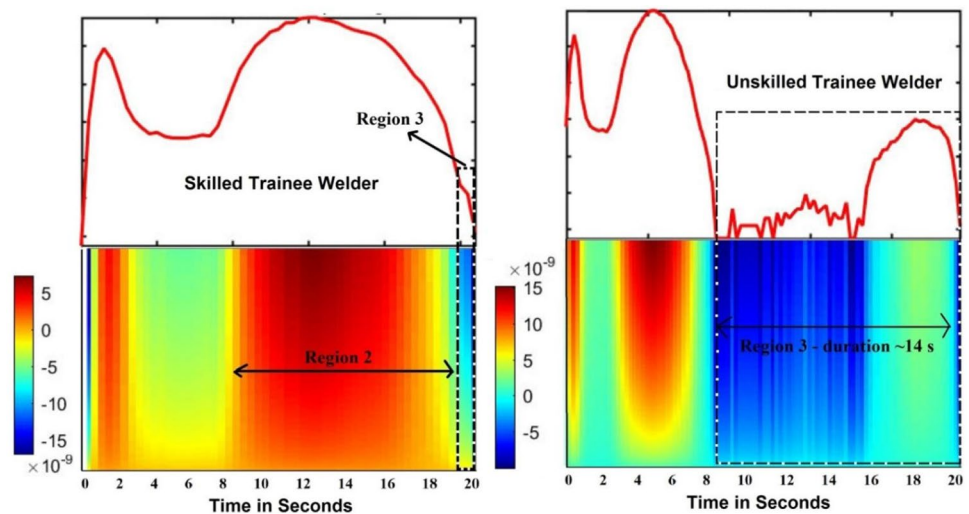


Table 2 Comparison of the welding skill using proposed method with its current practice

Welder ID	PDD rank region 2 (Kumar et al. 2018a)	Ranking by monitoring the welding dura- tion of region 2 (Using proposed method)	PDD rank region 3 (Kumar et al. 2018a)	Ranking by monitoring the welding duration of Region 3 (Using proposed method)
15	1	1	2	1
8	2	3	3	3
14	4	2	7	7
6	5	5	12	11
7	6	6	14	14
3	20	19	20	20
13	19	18	10	10
9	7	7	11	12
10	8	8	9	9
12	9	11	17	15
17	18	20	19	19
19	11	12	8	8
1	12	13	4	4
11	13	9	15	16
16	3	4	5	5
5	14	15	13	13
20	15	16	6	6
18	16	14	1	2
2	17	17	18	18
4	10	10	16	17

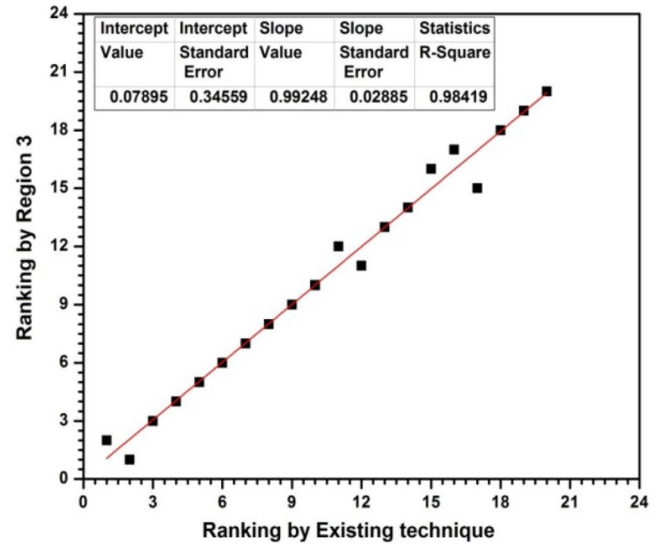
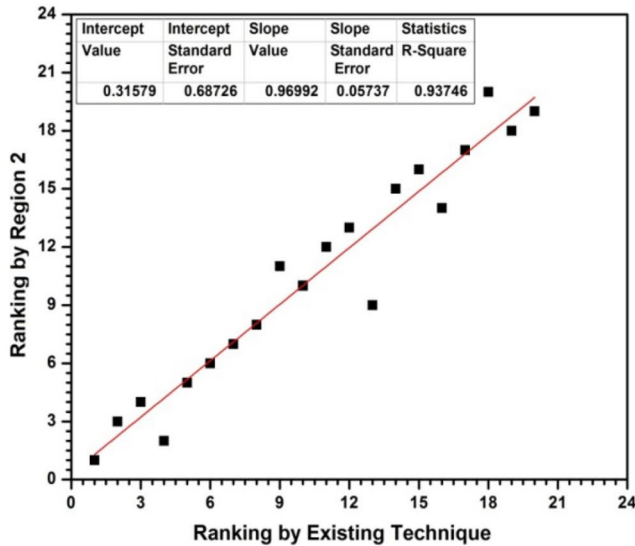


Fig. 7 Correlation between the ranks proposed by current and proposed methodology

electrodes was also observed to be around 1 s. These results were also correlated with the time domain analysis (Fig. 9) of the arc voltage signals acquired during the actual welding process and a very good correlation were observed between them.

4.3 Effect of shielding gases in GMAW process

In a GMAW Process, depending on the composition of shielding gases and current combinations, the metal transfer mechanism can be either short-circuiting, globular, or spray

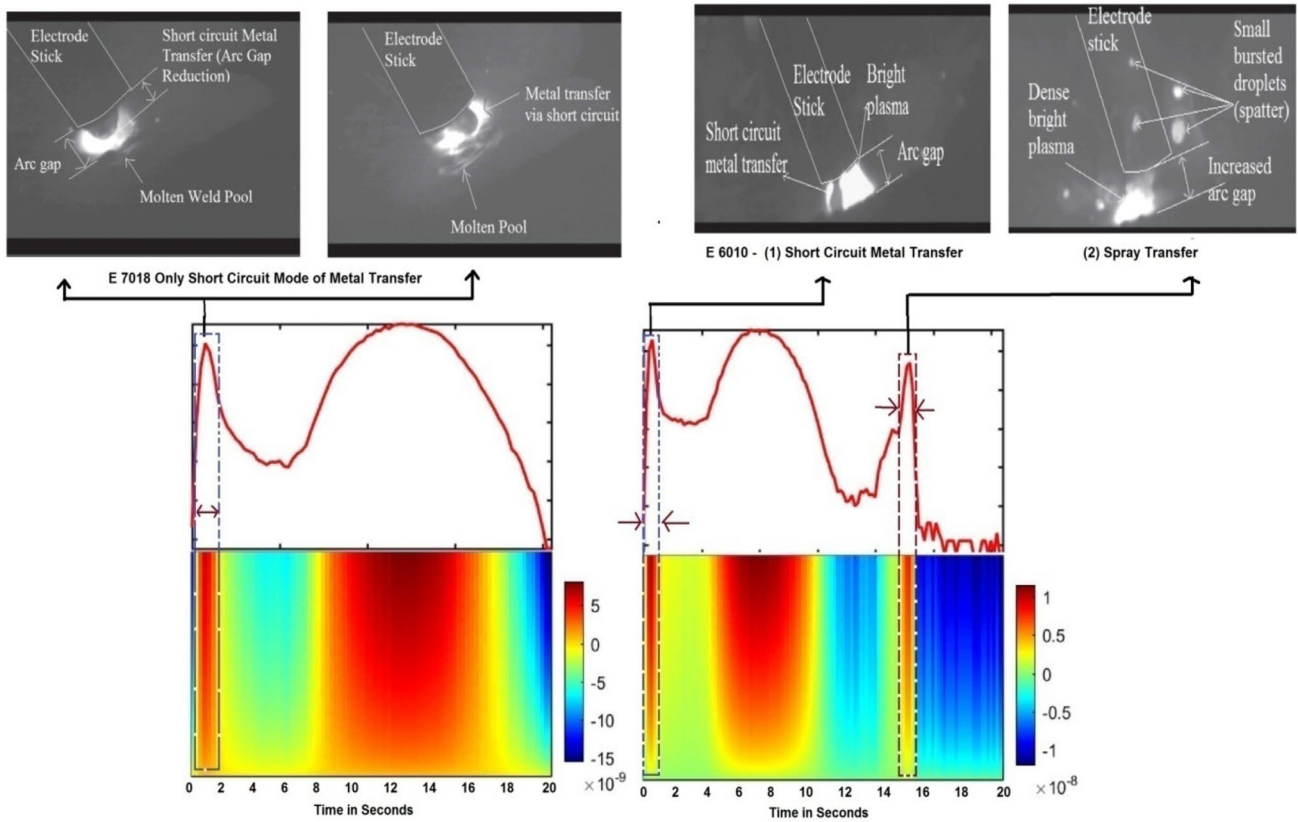


Fig. 8 CWT-FFT analysis of the voltage PDD and its correlation with pool image of (1) basic E 7018 and (2) cellulosic E 6010 electrodes

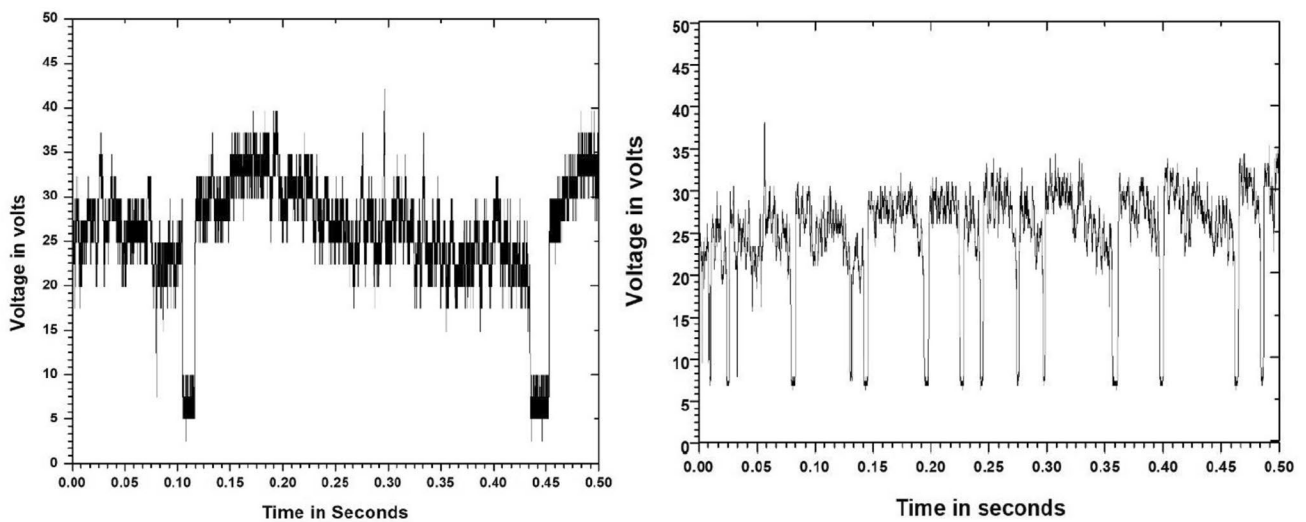


Fig. 9 Time-domain analysis of E 7018 and E 6010 electrodes

type (Kumar et al. 2018b). Therefore, to know their exact behavior, we have used different gas compositions (Table 1) to find out whether changing modes of metal transfer can be correlated with its corresponding voltage and current signal.

Figure 10 represents the scalogram (using CWT-FT method) of the voltage PDD obtained for GMAW-P when 80% Ar and 20% CO₂ gas composition was used. We can see from this figure that at around 200 A, the duration of the first peak (or

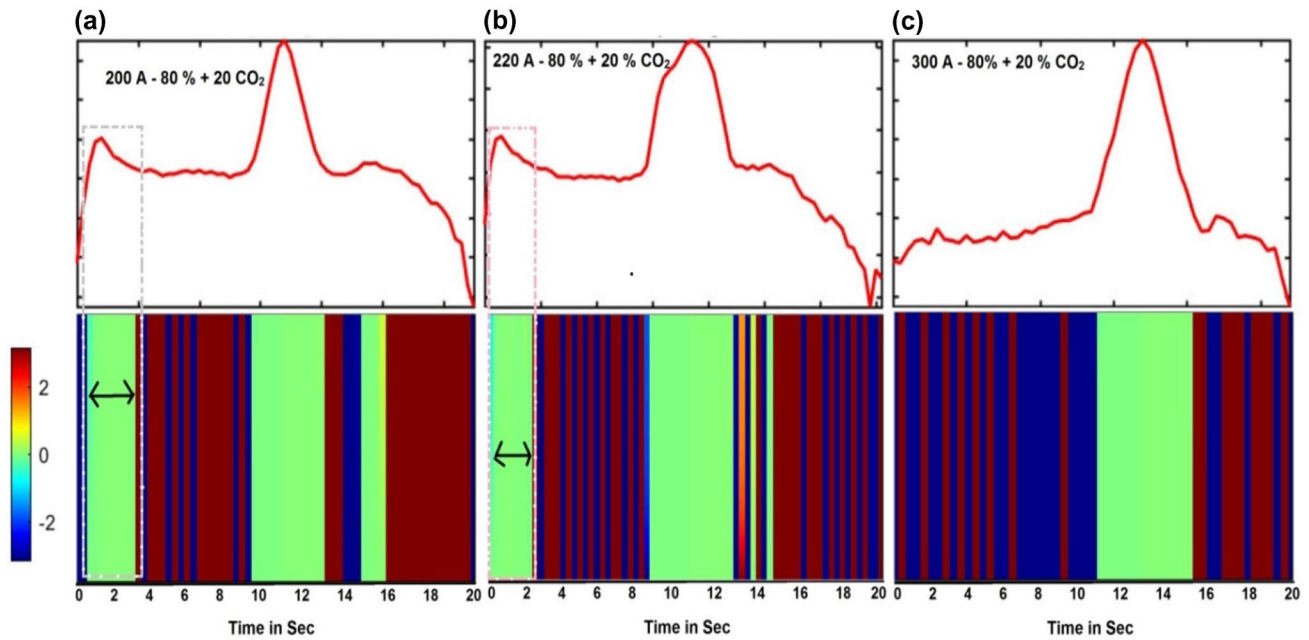


Fig. 10 CWT-FFT analysis of the voltage PDD of 80% Ar and 20% CO₂ shielding gas composition in GMAW process at **a** 200 A **b** 220 A and **c** 300 A

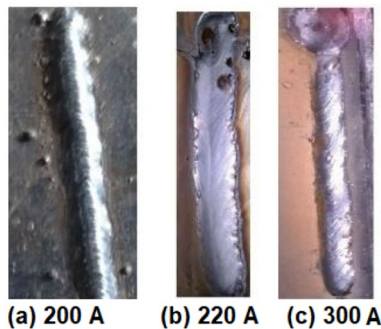


Fig. 11 Bead images of the weld from 80% Ar and 20% CO₂ shielding gas composition in GMAW process at **a** 200 A **b** 220 A and **c** 300 A

short circuit transfer) is around 3 s. Due to the considerable duration of short circuit metal transfer, a spatter of molten droplets around the welded area may occur before separating from the wire on account of a mild explosion that takes place due to an increased current (Kumar et al. 2018b). Therefore, many spatters can be noticed in its bead image shown in Fig. 11a. With increasing current (from 200 to 220 A) significant decrease in short circuit metal transfer duration was noticed (~2 s) and consequently, the spatter around the weld also decreased. With a further increase in current (at around 300 A), the first peak of voltage PDD or the short circuit metal transfer duration disappeared (Fig. 10c). Because for 80% Ar and 20% CO₂ gas composition, at around 300 A, spray mode of metal transfer start dominating (Kumar et al.

2018b). Note that spatter around the welded area has significantly decreased now (Fig. 11c). Results and the trends just now mentioned were in correlation with the time domain analysis of the shielding gas composition of 80% Ar and 20% CO₂ (see Fig. 13a).

Figure 12 show the scalogram obtained using CWT-FFT analysis of the voltage PDD plotted by maintaining the shielding gas composition to 100% Ar and by varying the current at three distinct levels (190 A, 220 A and 240 A). A comparison of these figures with the one obtained by varying the shielding gas to 80% Ar and 20% CO₂ gas mixtures (Fig. 10), indicates that the duration of the first peak (or short circuit metal transfer) decreases as the current increases from 190 to 240 A (~4 s at 190 A, ~2 s at 220 A and negligible duration at 240 A). This means that as the current increases from 190 to 240 A, short circuit transfer gradually changes to the globular transfer and then finally to spray transfer at around 240 A (Craig 1991). Readers should keep in mind that due to 100% Ar content; poor surface tension property may occur which may lead to very unstable and erratic welding characteristics (Ebrahimi et al. 2009; Kah and Martikainen 2013; O'Brien, welding hand book 1991). It may also be noted that although 100% Ar is not commonly used as a shielding gas in GMAW-P, this study has included the same to show how variations in arc characteristics caused by variations in shielding gas composition can be investigated by noticing the short circuit duration using CWT-FFT analysis technique. Results just now presented once again agree with the time domain analysis of

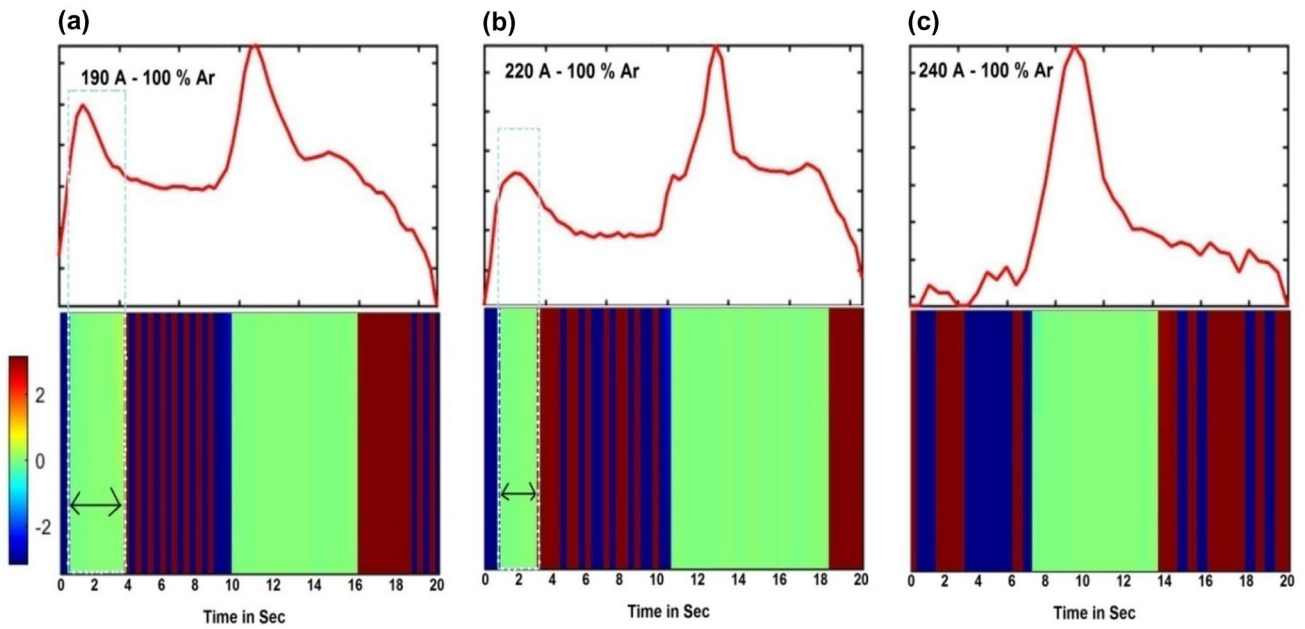


Fig. 12 Scalogram of voltage PDD of 100% Ar shielding gas in GMAW process at a 190 A b 220 A and c 240 A

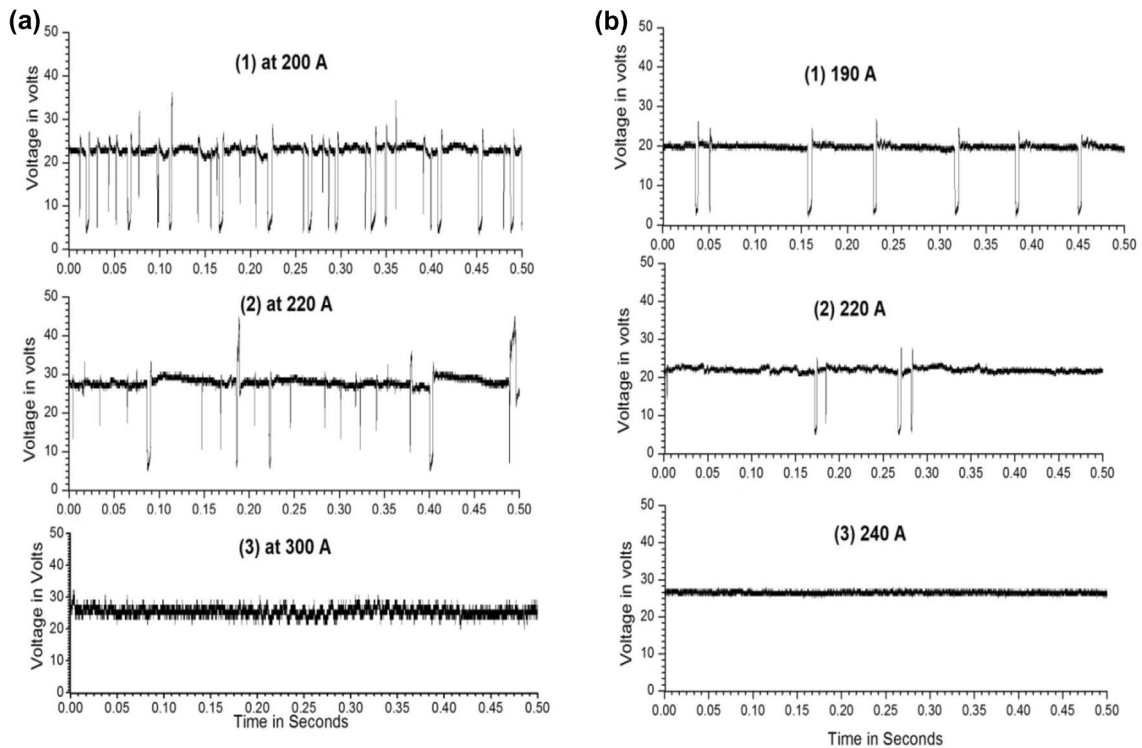


Fig. 13 Time domain analysis of a 80% CO₂ & 20% CO₂ shielding gas composition b 100% Ar in GMAW process

the 100% Ar shielding gas composition shown in Fig. 13b (Ebrahimnia et al. 2009).

Figure 14 and 15 shows the CWT-FFT of the voltage PDD and time domain analysis respectively of 100% CO₂

shielding gas composition at different current levels. A careful examination of these figures clearly indicates that irrespective of current magnitude the short circuit duration of voltage PDD in CWT-FFT analysis and voltage dips (in

Fig. 14 CWT-FFT analysis of the voltage PDD of 100% CO₂ shielding gas (1) at 150 A and (2) at 200 A

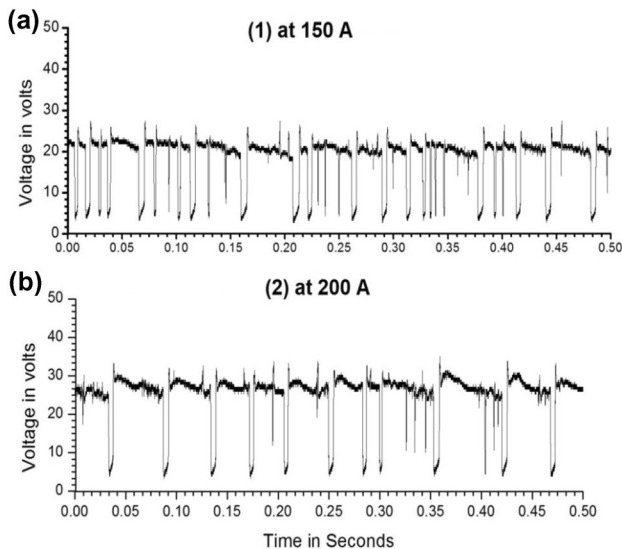
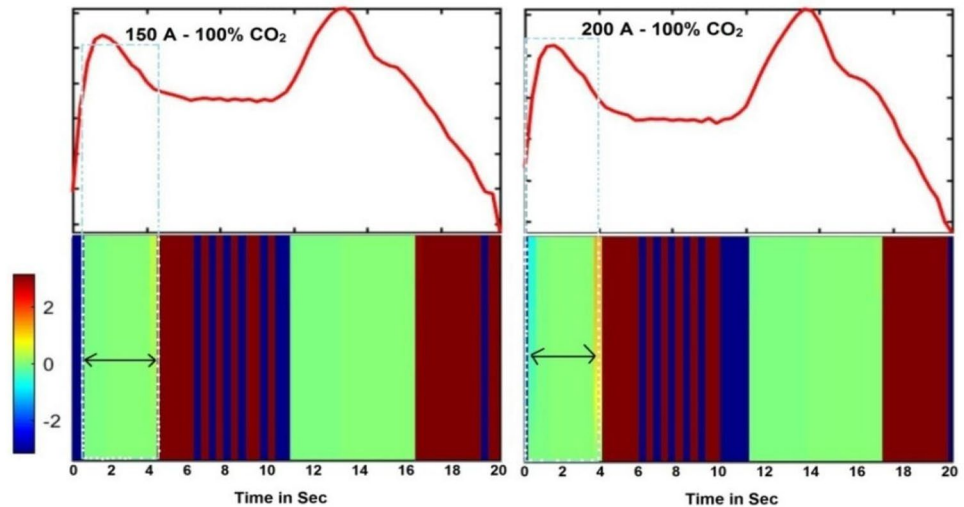


Fig. 15 Time domain analysis of a 100% CO₂ shielding gas at (1) 150 A and (2) 200 A in GMAW process

time domain analysis) almost remains the same. This means that only short circuit or globular modes of metal transfers are dominant modes in 100% CO₂ shielding gas, there is no spray transfer associated with 100% CO₂ shielding gas. The results were in agreement with conclusion drawn in O'Brien, welding hand book (1991) where the authors found that for more than 20% CO₂, spray mode of metal transfer is difficult to achieve.

It is evident from the above discussions that a CWT-FFT based analysis can be easily used to evaluate welding skill and welding consumables in a SMAW by monitoring the duration of various process parameters from the scalogram of their corresponding voltage PDD. Similarly, a CWT-FFT analysis can also be used to study the role of shielding gas composition on arc characteristics and the current above

which spray transfer occurs in a GMAW process. Practical implicants of the proposed CWT-FFT technique over traditional PDD techniques are significant because in contrast to a PDD analysis the proposed CWT-FFT have the potential to quantify the exact duration of an individual process parameter. For example, with the proposed analysis, one can easily find out the percentage variations of short circuit duration (or steady-state variations) between a skilled and an unskilled welder and once that is done a simple computer algorithm is sufficient to grade their welding skills. Similarly, with the help of the proposed CWT-FFT technique, the variations in the mode of metal transfers and its transition from one state to another with varying currents can also be evaluated with reasonable accuracy.

5 Conclusion

This research. This research underscores the application of Continuous Wavelet Transform–Fast Fourier Transform (CWT-FFT) technique in distinct contexts. It is implemented primarily to evaluate welding skills and appraise welding consumables within the Shielded Metal Arc Welding (SMAW) process. It's also employed to probe the ramifications of variable currents and shielding gases in the Gas Metal Arc Welding (GMAW) process. The results gleaned from this study corroborate the following conclusions:

1. CWT-FFT analysis proves instrumental in quantifying the durations of various regions within the voltage Probability Density Distributions (PDDs) of diverse trainee welders, serving as a potent grading tool for their welding skills. It is observed that the durations of steady-state welding and high voltage regions on voltage PDDs exhibit continuous improvement as the training of the welders progresses.

2. The proposed methodology renders a time and cost-efficient avenue for the evaluation of welding skills. It permits large-scale screening or grading of welders on construction sites, requiring only the acquisition of weld data from a bead-on-plate weld.
3. The CWT-FFT analysis demonstrates the capacity to differentiate and compare the performance of an array of welding consumables. It holds potential to distinguish between identical types of welding electrodes, manufactured from similar welding consumables by disparate manufacturers, thereby grading them based on their arc characteristics.

CWT-FFT is deployed to study the effects of combinations of shielding gases and currents within the GMAW process. The scalogram of the voltage PDD, obtained via the CWT-FFT technique, distinctly differentiates the mode of metal transfer when gas compositions and current combinations are altered.

Looking forward, our study opens several avenues for future research, which enhances the extensibility and applicability of our findings. One possible direction includes extending the CWT-FFT analysis to other types of welding processes, different types of electrodes, or varying welding conditions. This expanded scope will further elucidate the wide-ranging applicability of the CWT-FFT method across different welding scenarios. Another pivotal direction is to develop quantitative metrics based on the CWT-FFT analysis that can provide a numerical measure of the welding quality or performance. The establishment of such metrics will enhance the precision and reliability of assessing welding operations. Furthermore, the exploration of other wavelet functions or other signal analysis techniques, such as machine learning methods for the analysis of arc welding signals, can be undertaken. The incorporation of these advanced methods might provide even more robust and comprehensive insights into welding processes. Lastly, a comprehensive study could involve varying the welding current and arc voltage and observing their effects on the metal transfer behaviour. Such an in-depth examination would unravel the intricate interplay between these parameters, furthering our understanding of the nuanced aspects of welding operations. These proposed directions of future work signify the immense potential of the CWT-FFT methodology in the realm of welding research.

Acknowledgements The authors would like to thank Dr A. K. Bhaduri, Director, Indira Gandhi Centre for Atomic Research (IGCAR, Kalpakkam) and Central Workshop Division of IGCAR for their support and encouragement. The authors would also like to thank the Dean, School of Electronics Engineering (SOEE), Kalinga Institute of Industrial Technology (KIIT), Deemed to be University and our colleagues at KIIT for extending their genuine support to carry out this study.

Author contributions Conceptualization: VK and SKA; methodology: VK and MK; software: VK and SG; validation: VK and SKA; formal analysis: SG, VK and MKP; investigation: VK, SG and SKA; data curation: VK and SG; writing—original draft preparation: VK and SG; writing—review and editing: SKA and MKP; visualization and supervision: VK and SKA; project administration: SKA. All authors have read and agreed to the drafted version of the current manuscript.

Funding The authors received no financial support for this research.

Data availability The authors declare that the data and the material included in the manuscript are included as electronic supplement material and are available within this article.

Code availability Not applicable.

Declarations

Conflicts of interest The authors declare that there is no conflict of interest associated with this work.

Ethics approval One section of this study involves welder's skill classification, for this, the authors confirm that necessary permission from the institution (Indira Gandhi Centre for Atomic Research, Kalpakkam) was taken.

Consent to participate The authors declare that the consent from all the participating welders (involved in this study) were taken.

Consent for publication The authors (along with all the co-authors and whole team) approve the submission of this manuscript to be considered for publication to IJAMT. The authors have also agreed to online copy right transfer statement of the IJAMT (Springer).

References

- Ador welding limited (2008) Modern Arc Welding Technology. Oxford & MBH publishing Co. Pvt. Ltd., New Delhi, India
- Bitharas I, McPherson NA, McGhie W et al (2018) Visualisation and optimisation of shielding gas coverage during gas metal arc welding. *J Mater Process Technol* 255:451–462. <https://doi.org/10.1016/j.jmatprotec.2017.11.048>
- Caglar R (2012) Wavelet transform and current signature analysis for welding machine measurement. *J Vibroengineering* 14:805–812. <https://www.jvejournal.com/article/10638>.
- Chen B, Chen S (2010) Multi-sensor information fusion in pulsed GTAW based on fuzzy measure and fuzzy integral. *Assem Autom* 30(3):276–285. <https://doi.org/10.1108/01445151011061172>
- Chen SB, lv N, (2014) Research evolution on intelligentized technologies for arc welding process. *J Manuf Process* 16(1):109–122. <https://doi.org/10.1016/j.jmapro.2013.07.002>
- Craig (1991) Gas metal arc and Flux cored welding parameters, A unique approach to parameters, *Weld Quality and Weld Costs*.
- Das B, Pal S, Bag S (2016) A combined wavelet packet and Hilbert-Huang transform for defect detection and modelling of weld strength in friction stir welding process. *J Manuf Process* 22:260–268. <https://doi.org/10.1016/j.jmapro.2016.04.002>
- Ebrahimnia M, Goodarzi M, Nouri M, Sheikhi M (2009) Study of the effect of shielding gas composition on the mechanical weld

- properties of steel ST 37–2 in gas metal arc welding. *Mater Des* 30(9):3891–3895. <https://doi.org/10.1016/j.matdes.2009.03.031>
- He K, Zhou Z, Wang C, Li X (2016) Arc signal analysis of square wave alternating current submerged arc welding using local mean decomposition. *J Adv Mech Des Syst Manuf*. <https://doi.org/10.1299/jamdsm.2016jamdsm0104>
- Kah P, Martikainen J (2013) Influence of shielding gases in the welding of metals. *Int J Adv Manuf Technol* 64:1411–1421. <https://doi.org/10.1007/s00170-012-4111-6>
- Kapranov BI, Sutorikhin VA (2017) Remote acoustic emission monitoring of metal ware and welded joints. *IOP Conf Ser: Mater Sci Eng* 253:012005. <https://doi.org/10.1088/1757-899X/253/1/012005>
- Komorowski D, Pietraszek S (2015) The use of continuous wavelet transform based on the fast Fourier transform in the analysis of multi-channel Electrogastronomy recordings. *J Med System* 40(1):10. <https://doi.org/10.1007/s10916-015-0358-4>
- Kumar V, Albert SK, Chandrasekhar N, Jayapandian J (2018a) Evaluation of welding skill using probability density distributions and neural network analysis. *Measurement* 116:114–121. <https://doi.org/10.1016/j.measurement.2017.11.009>
- Kumar V, Albert SK, Chandrasekhar N, Jayapandian J (2018b) Performance evaluation of arc welding process using weld data analysis. *Trans Indian Inst Met* 71:3063–3075. <https://doi.org/10.1007/s12666-018-1450-5>
- Kumar V, Albert SK, Chandrasekhar N (2020) Development of programmable system on chip-based weld monitoring system for quality analysis of arc welding process. *Int J Comp Integr Manuf* 33(9):925–935. <https://doi.org/10.1080/0951192X.2020.1815847>
- Lanzoni M, Salomoni M, Riccò B (2010) Seam welding monitoring system based on real-time electrical signal analysis. *Weld J (miami, Fla)* 89:218S–223S
- Lebar A, Selak L, Vrabčič R, Butala P (2012) Online monitoring, analysis, and remote recording of welding parameters to the welding diary. *Strojnikski Vestnik-J Mech Eng* 58(7–8):444–452. <https://doi.org/10.5545/sv-jme.2012.341>
- Li ZY, Gao XD (2014) Study on regression model of measuring weld position. *Appl Mech Mater* 511–512:514–517. <https://doi.org/10.4028/www.scientific.net/AMM.511-512.514>
- Li X, Simpson S (2009) Parametric approach to positional fault detection in short arc welding. *Sci Technol Weld Join* 14(2):146–151. <https://doi.org/10.1179/136217108X370272>
- Luksa K, Rymarski Z (2006) Collection of arc welding process data. *J Achiev Mater Manuf Eng* 17:377–379
- Lv N, Xu Y, Zhang Z et al (2013) Audio sensing and modeling of arc dynamic characteristic during pulsed Al alloy GTAW process. *Sensor Rev* 33(2):141–156. <https://doi.org/10.1108/0260228131299680>
- Martínez RT, Alfaro SCA (2020) Data analysis and modeling techniques of welding processes: the state-of-the-art. *Intech Open Welding-Modern topics* pp 1–25
- Mirapeix J, Cobo A, Fuentes J et al (2009) Use of the plasma spectrum RMS signal for arc-welding diagnostics. *Sensors* 9(7):5263–5276. <https://doi.org/10.3390/s90705263>
- O'Brien, welding hand book (1991) 8th Edition volume 2, welding process, American Welding Society.
- Pal S, Pal SK, Samantaray, (2010) Determination of optimal pulse metal inert gas welding parameters with a neuro- GA technique. *Mater Manuf Process* 25:606–615. <https://doi.org/10.1080/10426910903179963>
- Rioul O, Vetterli M (1991) Wavelets and signal processing. *IEEE Signal Process Mag* 8:14–38. <https://doi.org/10.1109/79.91217>
- Shin S, Jin C, Yu J, Rhee S (2020) Real-time detection of weld defects for automated welding process base on deep neural network. *Metals* 10(3):389. <https://doi.org/10.3390/met10030389>
- Siewert T, Samardžić I, Klaric S (2002) Application of an on-line weld monitoring system. *Proc 1st DAAAM Int Conf Adva Tech Dev Countries* 227–232. <https://www.bib.irb.hr/76583?rad=76583>.
- Song H, Zhang Y (2007) Three-dimensional reconstruction of specular surface for a gas tungsten arc weld pool. *Meas Sci Technol* 18:3751–3767. <https://doi.org/10.1088/0957-0233/18/12/010>
- Torrence C, Compo GP (1998) A practical guide to wavelet analysis. *Bull Am Meteorol Soc* 79:61–78. [https://doi.org/10.1175/1520-0477\(1998\)079%3c0061:APGTWA%3e2.0.CO;2](https://doi.org/10.1175/1520-0477(1998)079%3c0061:APGTWA%3e2.0.CO;2)
- Yang L, Jiang H (2020) Weld defect classification in radiographic images using unified deep neural network with multi-level features. *J Intell Manuf* 32(2):459–469
- Yu W, Dalu G, Mingfu L (2005) A better method for detecting friction welding defect. *J Northwestern Polytech Univ* 23(4):496–499
- Zhang Z, Chen H, Xu Y et al (2015) Multisensor-based real-time quality monitoring by means of feature extraction, selection and modeling for Al alloy in arc welding. *Mech Syst Signal Process* 60:151–165. <https://doi.org/10.1016/j.ymssp.2014.12.021>
- Zhang S, Hu S, Wang Z (2016) Weld penetration sensing in pulsed gas tungsten arc welding based on arc voltage. *J Mater Process Technol C* 229:520–527. <https://doi.org/10.1016/j.jmatprotec.2015.09.034>
- Zhang B, Shi Y, Gu S (2018) Narrow-seam identification and deviation detection in keyhole deep-penetration tig welding. *Int J Adv Manuf Technol* 101:2051–2064. <https://doi.org/10.1007/s00170-018-3089-0>
- Zhang L, Basantes A, Ozevin D, Indacochea E (2019) Real-time monitoring of welding process using air-coupled ultrasonics and acoustic emission. *Int J Adv Manuf Technol* 101(5):1623–1634. <https://doi.org/10.1007/s00170-018-3042-2>
- Zhou W, Li Q, Zhou Z (2001) Power quality detection using wavelet-Multiresolution signal decomposition. *Trans China Electrotech Soc* 16(6):81–84. <https://doi.org/10.1080/00051144.2019.1565337>

Publisher's Note Springer Nature remains neutral with regard to jurisdictional claims in published maps and institutional affiliations.

Springer Nature or its licensor (e.g. a society or other partner) holds exclusive rights to this article under a publishing agreement with the author(s) or other rightsholder(s); author self-archiving of the accepted manuscript version of this article is solely governed by the terms of such publishing agreement and applicable law.